DOI: 10.1002/cjoc.201200091

Ethoxy-substituted Oligo-phenylenevinylene-Bridged Organic Dyes for Efficient Dye-Sensitized Solar Cells

Shan, Yifan[a](单益凡)　Tang, Jie[a](汤杰)　Lai, Hua[b](赖华)　Tan, Hongwei[c](谭宏伟)
Liu, Xiaofeng[d](刘晓峰)　Yang, Fan*,[a](杨帆)　Fang, Qiang*,[b](房强)

[a] *Institutes for Advanced Interdisciplinary Research, East China Normal University, Shanghai 200062, China*
[b] *Shanghai Institute of Organic Chemistry, Chinese Academy of Sciences, Shanghai 200032, China*
[c] *Department of Chemistry, Beijing Normal University, Beijing 100875, China*
[d] *Reata Pharmaceuticals, Inc. 2801 Gateway Drive, Suite 150, Irving, Texas 75063, USA*

Organic dyes with ethoxy-substituted oligo-phenylenevinylene as chromophores were synthesized for dye-sensitized solar cells (DSSCs), and the detailed relationships between the dye structures, photophysical properties, electrochemical properties, and performances of DSSCs were described. The dye S3O showed broad IPCE spectra in the spectral range of 350—750 nm, and the dye S1P showed solar energy-to-electricity conversion efficiency (η) of up to 4.23% under AM 1.5 irradiation (100 mW/cm^2) in comparison with the reference Ru-complex (N719 dye) with an η value of 5.90% under similar experimental conditions.

Keywords dye-sensitized solar cell, organic dyes, ethoxy-substituted oligo-phenylenevinylene, photovoltaic, synthesis

Introduction

Dye-sensitized solar cells (DSSCs) based on Ru dyes have been actively investigated since Grätzel and co-workers reported the first photoelectric device with highly efficient solar-energy-to-electricity conversion efficiencies of 11% under AM 1.5 irradiation.[1-7] In addition to Ru complexes, metal-free organic dyes have also been utilized as photosensitizers in DSSCs because of their wide variety of the structures, facile modification, high molar absorption coefficient, low cost, and environment-friendliness.[8-26] And impressive device efficiencies of 9%—10% have been achieved based on organic dyes. It is very instructive that porphyrin-sensitized solar cells with cobalt(II/III)-based redox electrolyte with exceed 12.3% efficiency was reported by Grätzel and co-workers in 2011.[27]

Generally, organic dyes should contain a structure of donor (D)-to-acceptor (A) bridged by a π-conjugation system and possess a broad and intense spectral absorption. Appropriate use of electron-excessive chains as π-conjugation between an electron donor and an electron acceptor was reported to be beneficial to red shift the charge-transfer transition. It was suggested that the efficiency of the DSSCs could be increased by introducing alkyl chains in the linker or donor part of the dye, which prevents the recombination of electrons from the semiconductor to the electrolyte by forming an insulating layer and yielding an increased electron lifetime. The alkyl chains are also believed to prevent aggregate formation on the surface of the TiO_2. The ethoxy groups also have been introduced at the phenylenevinylene moiety to enhance the electron donating character and introduced into the π-conjugated donor-acceptor skeleton to increase the absorption wavelength.[28]

Herein, we report three new organic dyes which contain a simple triphenylamine or dibutoxy-substituted triphenylamine moiety or phenoxazine unit as the electron donor and cyanoacrylic acid as the electron acceptor. The donor and acceptor are bridged by ethoxy-substituted oligo-phenylenevinylene which serves as a coplanar π-conjugated spacer to give three organic D-π-A dyes S1P, S3O and S3P (Figure 1).

Experimental

Absorption spectra in CH_2Cl_2 solutions were recorded in a quartz cell with 1 cm path length on Varian Cary 100 Bio UV-Visible spectrophotometer. Fluorescent spectra were recorded on Hitachi F-4500. ^{1}H NMR (500 MHz) and ^{13}C NMR (125 MHz) spectra were measured with Bruker AM-500 MHz, with the chemical shifts against TMS. MS data were obtained with Bruker micrOTOF II. Electrochemical redox potentials were obtained by cyclic voltammetry (CV) using a three-

---

* E-mail: fyang@chem.ecnu.edu.cn (F. Yang), qiangfang@mail.sioc.ac.cn (Q. Fang); Tel.: 0086-021-62232764; Fax: 0086-021-62232100

Received February 7, 2012; accepted April 1, 2012.
Supporting information for this article is available on the WWW under http://dx.doi.org/10.1002/cjoc.201200091 or from the author.

© 2012 SIOC, CAS, Shanghai, & WILEY-VCH Verlag GmbH & Co. KGaA, Weinheim

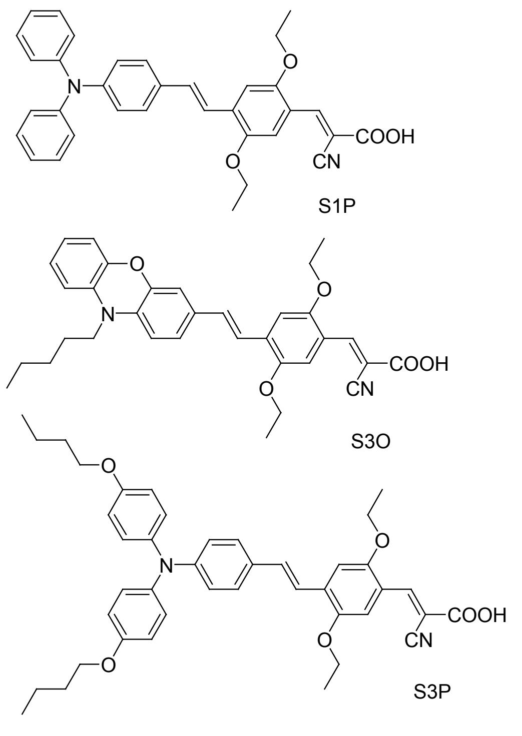

Figure 1 The molecular structures of all dyes.

electrode cell and an electrochemistry workstation (CHI600C). The working electrode was a glass carbon electrode; the auxiliary electrode was a Pt wire and Ag/AgI/I^- was used as reference electrode. 0.1 mol/L tetrabutylammonium hexaflourophosphate ($TBAPF_6$) was used as supporting electrolyte in CH_2Cl_2. Ferrocene was added to each sample solution at the end of the experiments and the ferrocenium/ferrocene (F_c/F_c^+) redox couple was used as an internal potential reference. The potentials versus NHE were calibrated by addition of 0.55 V to the potentials versus F_c/F_c^+. Unless otherwise stated, starting materials were used as commercially purchased without further purification. The syntheses route of S1P, S3O and S3P are shown in Scheme 1.

The intermediate 2,5-diethoxyterephthalaldehyde was prepared according to literature procedures.[29,30]

Synthesis of S1P-CHO

To a solution of 2,5-diethoxyterephthalaldehyde (0.85 g, 3.85 mmol) and compound **1** (2.31 g, 3.85 mmol) in 35 mL THF, *t*-BuOK (0.65 g, 5.78 mmol) was added slowly with vigorously stirring at room temperature. The reaction was completed within 3 h. The reaction mixture was poured into water and filtered to collect the orange solid (a mixture of *E* and *Z* isomers), which was then dried *in vacuo*. Then the dry solid was dissolved in 35 mL THF to reflux in the presence of catalysis amount iodine for 8 h. The mixture was added sodium bisulfite aqueous solution to remove iodine, then extracted with dichloromethane. Organic layer was dried with anhydrous sodium sulfate and removed the solvent, and was purified by column chromatography using silica gel and dichloromethane-petroleum ether (1/1, *V*/*V*) as the eluent to give S1P-CHO (yellow solid, *E*, 0.78 g, yield 44%); ^1H NMR (500 MHz, $CDCl_3$) δ: 1.45 (t, $J=7.0$ Hz, 3H), 1.48 (t. $J=7.0$ Hz, 3H), 4.09 (q, $J=7.0$ Hz, 2H), 4.19 (q, $J=7.0$ Hz, 2H), 7.04—7.06 (m, 4H), 7.11—7.13 (m, 4H), 7.16—7.19 (m, 2H), 7.26—7.27 (m, 4H), 7.29 (s, 1H), 7.31—7.34 (m, 1H), 7.41—7.43 (m, 2H), 10.43 (s, 1H); ^{13}C NMR (125 MHz, $CDCl_3$) δ: 189.0, 156.1, 150.4, 147.9, 147.3, 134.7, 131.7, 131.0,

Scheme 1 Synthetic routes of S1P, S3O and S3P

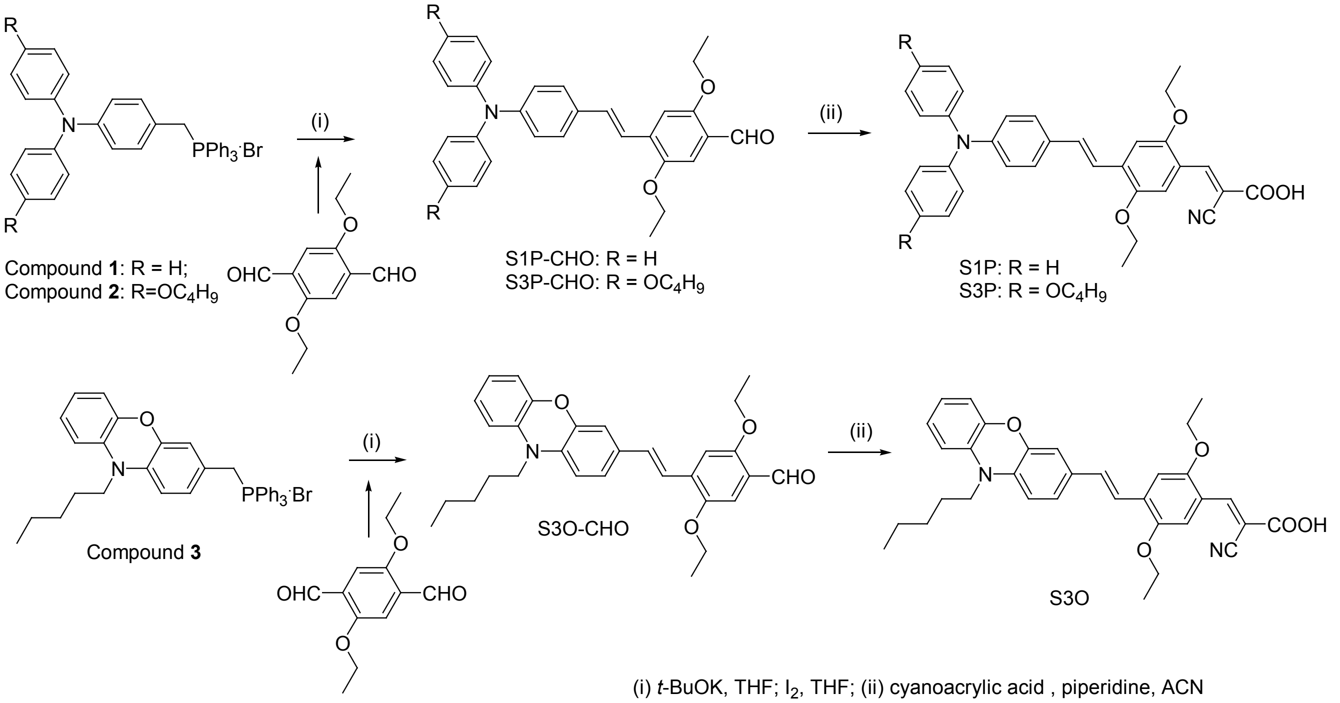

(i) *t*-BuOK, THF; I_2, THF; (ii) cyanoacrylic acid , piperidine, ACN

© 2012 SIOC, CAS, Shanghai, & WILEY-VCH Verlag GmbH & Co. KGaA, Weinheim

129.3 (4C), 127.8 (2C), 124.7 (4C), 124.4, 123.9, 123.3 (2C), 123.0 (2C), 120.9, 110.2, 110.1, 64.8, 64.5, 14.8 (2C). HRMS (ESI) calcd for $C_{31}H_{29}NNaO_3$ $[M+Na]^+$ 486.2045, found 486.2056.

Synthesis of S1P

An acetonitrile (10 mL) solution of S1P-CHO (0.10 g, 0.22 mmol) and cyanoacetic acid (22 mg, 0.26 mmol) was refluxed in the presence of piperidine (0.10 mL) for 2 h. After removing the solvent, the residue was purified by column chromatography using silica gel and dichloromethane-methanol (10/1, *V*/*V*) as the eluent to give product S1P (dark-red solid, 70 mg, yield 60%). m.p. 248—252 ℃; ^{1}H NMR (500 MHz, $CDCl_3$) δ: 1.47—1.49 (m, 6H), 4.12—4.19 (m, 4H), 7.05—7.07 (m, 4H), 7.12 (d, J=7.1 Hz, 5H), 7.19 (d, J=16.6 Hz, 1H), 7.26—7.30 (m, 4H), 7.36 (d, J=16.3 Hz, 1H), 7.42 (d, J=8.4 Hz, 2H), 7.96 (s, 1H), 8.77 (s, 1H); ^{13}C NMR (125 MHz, $CDCl_3+CD_3OD$) δ: 183.90, 164.81, 153.54, 149.98, 148.64, 147.89, 147.13 (2C), 134.17, 131.70, 130.77, 129.11 (4C), 127.69 (2C), 124.56 (4C), 123.14 (2C), 122.71 (2C), 120.49, 119.58, 116.90, 111.42, 109.19, 64.82, 64.55, 14.48, 14.40. HRMS (ESI) calcd for $C_{34}H_{30}N_2NaO_4$ $[M+Na]^+$ 553.2098, found 553.2086.

Synthesis of S3O-CHO

Compound S3O-CHO was synthesized according to the same procedure as that of S1P-CHO except that compound **3** (2.34 g, 3.85 mmol) was used instead of compound **1**. Yellow solid of S3O-CHO was obtained in 70% yield. ^{1}H NMR (500 MHz, $CDCl_3$) δ: 0.97 (t, J=7.0 Hz, 3H), 1.42—1.44 (m, 4H), 1.48 (t, J=7.0 Hz, 3H), 1.50 (t, J=7.0 Hz, 3H), 1.67—1.73 (m, 2H), 3.50 (t, J=8.5 Hz, 2H), 4.11 (q, J=7.0 Hz, 2H), 4.20 (q, J=7.0 Hz, 2H), 6.45 (d, J=8.3 Hz, 1H), 6.50 (d, J=8.2 Hz, 1H), 6.66—6.70 (m, 2H), 6.81—6.84 (m, 1H), 6.91 (s, 1H), 6.94 (d, J=8.2 Hz, 1H), 7.03 (d, J=16.4 Hz, 1H), 7.14 (s, 1H), 7.25 (d, J=16.4 Hz, 1H), 7.32 (s, 1H), 10.44 (s, 1H); ^{13}C NMR (125 MHz, $CDCl_3$) δ: 189.06, 156.07, 150.36, 145.05, 144.69, 134.72, 133.55, 132.59, 131.32, 130.17, 123.79, 123.69 (2C), 121.08, 120.06, 115.38, 112.46, 111.40, 111.02, 110.12, 110.00, 64.81, 64.51, 44.08, 29.04, 24.73, 22.49, 14.86, 14.79, 14.06. HRMS (ESI) calcd for $C_{30}H_{33}NNaO_4$ $[M+Na]^+$ 494.2307, found 494.2312.

Synthesis of S3O

Compound S3O was synthesized according to the same procedure as that of S1P except that S3O-CHO (0.10 g, 0.22 mmol) was used instead of S1P-CHO. Red solid of S3O was obtained in 46% yield. m.p. 258—260 ℃; ^{1}H NMR (500 MHz, $CDCl_3+CD_3OD$) δ: 0.93 (t, J=6.6 Hz, 3H), 1.40 (m, 4H), 1.45—1.49 (m, 6H), 1.66 (m, 2H), 3.49 (m, 2H), 4.10—4.16 (m, 4H), 6.43 (d, J=8.0 Hz, 1H), 6.48 (d, J=8.2 Hz, 1H), 6.64 (m, 2H), 6.78—6.80 (m, 1H), 6.88 (s, 1H), 6.92 (d, J=8.2 Hz, 1H), 7.03—7.08 (m, 2H), 7.23 (d, J=17.0 Hz, 1H), 7.92 (s, 1H), 8.73 (s, 1H); ^{13}C NMR (125 MHz, DMSO-d_6) δ: 163.74, 152.91, 149.35, 146.33, 144.22, 143.83, 133.21, 133.07, 132.11, 131.54, 129.90, 124.00, 123.92, 121.03, 119.45, 117.09, 117.09, 115.01, 111.95, 112.03, 111.80, 111.32, 110.20, 107.82, 64.70, 64.28, 43.00, 28.19, 24.22, 21.83, 14.48 (2C), 13.78. HRMS (ESI) calcd for $C_{33}H_{34}N_2NaO_5$ $[M+Na]^+$ 561.2365, found 561.2377.

Synthesis of S3P-CHO

Compound S3P-CHO was synthesized according to the same procedure as that of S1P-CHO except that compound **2** (2.86 g, 3.85 mmol) was used instead of compound **1**. Yellow solid of S3P-CHO was obtained in 48% yield. ^{1}H NMR (500 MHz, $CDCl_3$) δ: 0.97 (t, J=7.0 Hz, 6H), 1.42—1.51 (m, 10H), 1.74—1.77 (m, 4H), 3.92 (t, J=5.0 Hz, 4H), 4.05—4.09 (m, 2H), 4.15—4.19 (m, 2H), 6.81 (d, J=8.5 Hz, 4H), 6.88 (d, J=8.5 Hz, 2H), 7.04 (d, J=9.0 Hz, 4H), 7.12—7.15 (m, 2H), 7.28—7.31 (m, 2H), 7.33 (d, J=8.5 Hz, 2H), 10.41 (s, 1H); ^{13}C NMR (125 MHz, $CDCl_3$) δ: 198.07, 156.12, 155.71 (2C), 150.28, 148.96, 140.18 (2C), 135.04, 132.02, 128.93, 127.69 (2C), 126.83 (4C), 123.62, 119.75 (2C), 119.67, 115.24 (4C), 110.02, 109.91, 67.88 (2C), 64.77, 64.50, 31.35 (2C), 19.23 (2C), 14.80, 14.77, 13.83 (2C). HRMS (ESI) calcd for $C_{39}H_{45}NNaO_5$ $[M+Na]^+$ 630.3195, found 630.3254.

Synthesis of S3P

Compound S3P was synthesized according to the same procedure as that of S1P except that S3P-CHO (0.13 g, 0.22 mmol) was used instead of S1P-CHO. Red solid of S3P was obtained in 40% yield. m.p. 246—248 ℃; ^{1}H NMR (500 MHz, $CDCl_3$) δ: 0.98 (t, J=7.6 Hz, 6H), 1.46—1.54 (m, 10H), 1.75—1.80 (m, 4H), 3.94 (t, J=6.4 Hz, 4H), 4.13—4.19 (m, 4H), 6.83 (d, J=8.8 Hz, 4H), 6.89 (d, J=8.6 Hz, 2H), 7.06—7.11 (m, 5H), 7.18 (d, J=16.2 Hz, 1H), 7.30—7.37 (m, 3H), 7.99 (s, 1H), 8.83 (s, 1H); ^{13}C NMR (125 MHz, $CDCl_3+CD_3OD$) δ: 177.56, 165.01, 155.49, 153.56, 149.84, 148.49, 140.05, 140.01, 134.47, 131.96, 127.57 (2C), 126.64 (4C), 119.52 (2C), 119.29 (2C), 117.00, 115.13 (4C), 112.01, 111.37 (2C), 108.92 (2C), 67.81 (2C), 64.76, 64.52, 31.10 (2C), 18.95 (2C), 14.43, 14.34, 13.45 (2C). HRMS (ESI) calcd for $C_{42}H_{46}N_2NaO_6$ $[M+Na]^+$ 697.3248, found 697.3233.

DSSCs fabrication

Titania paste was prepared from P25 (Degussa, Germany) following the literature procedure[2] and deposited onto the F-doped tin oxide conducting glass (sheet resistance of 15 Ω/square, polyethylene naphthalate) by doctor-blading. The resulted layer photoelectrode of 12 μm thickness, was sintered at 500 ℃ for 30 min in air. After the film was cooled to 40 ℃, it was immersed into a 3×10^{-4} mol/L dye solution in THF and maintained under dark for 12 h. The electrode was then rinsed with CH_2Cl_2 and dried. One drop of electrolyte solution was deposited onto the surface of the electrode and penetrated inside the TiO_2 film via capillary action. The electrolyte consisted of 1.0 mol/L 1,2-dimethyl-3-*n*-propylimidazolium iodide (DMPII), 0.05 mol/L LiI, 0.03 mol/L I_2, 0.1 mol/L guanidinium thiocyanate (GuSCN), 0.5 mol/L 4-*tert*-butylpyridine (TBP) in AcCN and valeronitrile (85∶15) for our dyes and N719 dye. A platinized counter electrode was then clipped onto the top of the TiO_2 working electrode to form our test cell.

The irradiance source was a 150 W NREL traceable Oriel Class AAA solar simulator (Model 92250A-1000). The output power was calibrated by a NREL traceable monocrystalline silicon reference cell (PVM 191) coupled with Newport Oriel PV reference cell system (Model 91150). Current-voltage characteristics were measured using a Keithley 2420 sourcemeter. The measurement delay time was fixed to 40 ms with 100 measurement points scanning from V_{OC} to J_{SC}.[31] For the setup used in our measurements, there was no hysteresis in the IV curves when reversing the scan direction.

Incident photon-to-current conversion efficiency (IPCE) of the DSSCs was measured by a DC method. The light source was a 300 W Xenon Lamp (Oriel 6285) coupled with a flux controller to improve the stability of the irradiance. The light passed through a monochromator (Cornerstone 260 Oriel 74125) to select a single wavelength with a resolution of 10 nm. The monochromatic light beam was then focused on the active region of the device. Light intensity was measured by a NREL traceable Si detector (Oriel 71030NS) and the short circuit currents of the DSSCs were measured by an optical power meter (Oriel 70310). The IPCE was calculated by the equation: $\text{IPCE}(\lambda) = 1240 \times J_{sc}(\lambda)/\lambda \times P_{in}(\lambda)$.

Results and Discussion

Upon condensation of SiP-CHO or S3O-CHO or S3P-CHO with cyanoacetic acid, respectively, by Knoevenagel reaction in the presence of piperidine, the target dyes were obtained conveniently. The geometric structure of these type of compound with cyanoacrylic acid as the acceptor/anchor group, has been investigated by Zhang *et al.*[33] through X-ray analysis.

Photophysical properties

The absorption spectra of S1P, S3O and S3P dyes in CH_2Cl_2 and on TiO_2 films are shown in Figure 2, and the corresponding data were collected in Table 1. All of dyes (S1P, S3O and S3P) have a relatively broad and strong absorption in the visible region with a maximum at 478, 509 and 507 nm, respectively. These absorption bands at around 500 nm can be attributed to the intramolecular charge transfer (ICT) between the donor and the acceptor. The molar extinction coefficients of S1P, S3O and S3P are 35 300 $dm^3 \cdot mol^{-1} \cdot cm^{-1}$ (478 nm), 33 200 $dm^3 \cdot mol^{-1} \cdot cm^{-1}$ (509 nm) and 39 500 $dm^3 \cdot mol^{-1} \cdot cm^{-1}$ (507 nm), respectively. These numbers are obviously larger than that of N719, indicating that these dyes have good light-harvesting ability. The absorption spectra of the modified donor series show that the longer alkoxy moieties of S3P red shift the absorption maximum when compared to S1P. Due to strong electron donating ability of phenoxazine (POZ) unit, S3O dye exhibits λ_{abs} at 509 nm which is similar to the absorption maximum of S3P. When S1P, S3O and S3P were sensitized on TiO_2 surface, the absorption maxima of these dyes were blue-shifted by 24, 54 and 58 nm in comparison to those in solution respectively, due to H-aggregation on semiconductor surface.

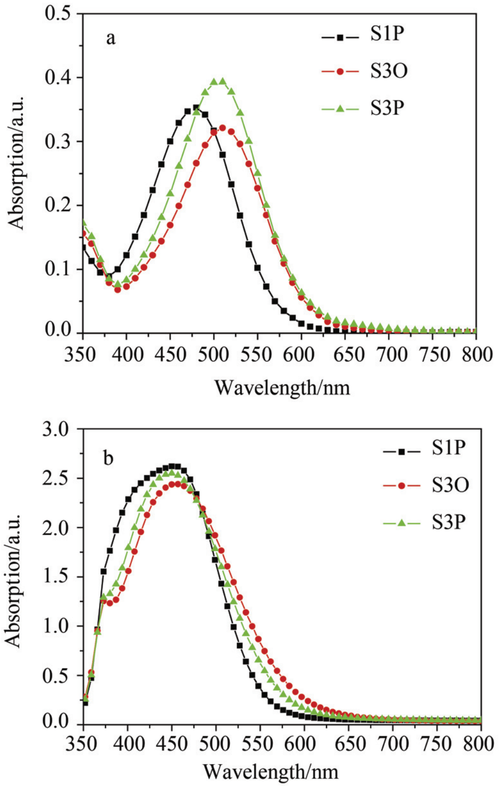

Figure 2 (a) Absorption spectra of S1P, S3O and S3P in CH_2Cl_2 (1×10^{-5} mol/L); (b) Absorption spectra of S1P, S3O and S3P on TiO_2 films.

Electrochemical properties

To further study the possibilities of electron injection from the dye in excited state to conduction band (CB) of the semiconductor and the dye regeneration, CVs of these dyes were performed in CH_2Cl_2 to measure the redox potentials (Figure 3). The first oxidation potentials (E_{ox}) corresponding to the HOMO levels of the dyes were summarized in Table 1. The HOMO levels of S1P, S3O and S3P dyes are 1.12, 0.73 and 0.77 V, respectively, which are positive enough compared to that of iodine/iodide (0.4 V),[32] therefore the oxidized dyes could be reduced effectively by electrolyte and regenerated (Figure 4). Compared to S1P, the additional butoxy groups in S3P result in a red-shift of the absorption and

© 2012 SIOC, CAS, Shanghai, & WILEY-VCH Verlag GmbH & Co. KGaA, Weinheim

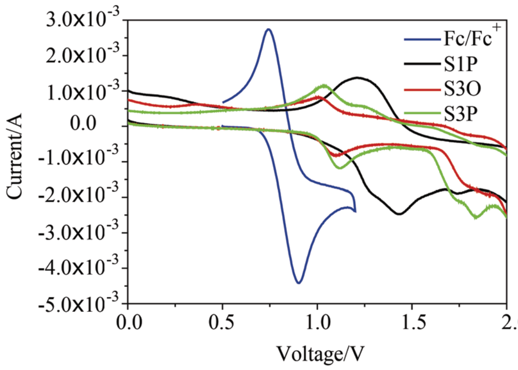

Figure 3 The CV curves of dyes in CH_2Cl_2.

Table 1 Absorption, emission, and electrochemical properties of S1P, S3O and S3P

Dye	Absorption		Oxidation potential data^c		
	$\lambda_{max}{}^a$/nm [ε/(L•mol^{-1}•cm^{-1})]	$\lambda_{max}{}^b$/nm on TiO_2	$E_{0\text{-}0}{}^d$/V	E_{ox}/V	($E_{ox}-E_{0\text{-}0}$)/V
S1P	478 (35 300)	454	2.17	1.12	−1.05
S3O	509 (32 200)	455	2.35	0.73	−1.62
S3P	505 (39 500)	447	2.22	0.77	−1.45

[a] Maximum absorption was measured in CH_2Cl_2 solution (1×10^{-5} mol/L) at room temperature; [b] Maximum absorption on TiO_2 film; [c] The oxidation potentials of the dyes were measured in CH_2Cl_2 with 0.1 mol/L tetrabutylammonium hexafluorophosphate ($TBAPF_6$) as electrolyte (working electrode: glassy carbon; reference electrode: Ag/AgI/I^-; calibrated with ferrocene/ferrocenium ($F_c/F_c{}^+$) as an internal reference, counter electrode: Pt); [d] $E_{0\text{-}0}$ was estimated from the onset point of absorption spectra.

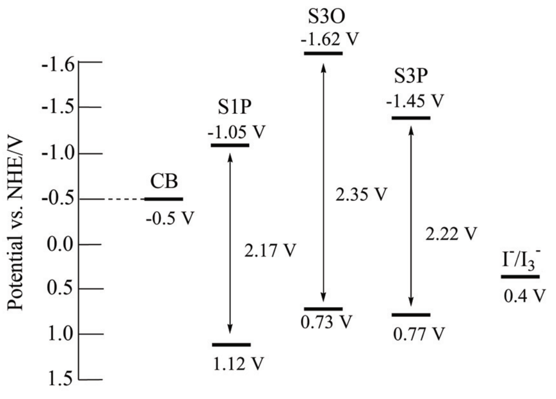

Figure 4 Molecular orbital energy diagram of HOMO and LUMO of dyes.

an increase of the 0-0 excitation energy ($E_{0\text{-}0}$) estimated from the absorption onset. The first oxidation potential of S1P is 1.12 V, but it shifts negatively by *ca.* 350 mV for S3P. The phenomena can be attributed to the electron-donating butoxy groups which raise the HOMO potential and reduce the coulombic repulsion between the two charges. The LUMO levels of these dyes can be obtained by HOMO level and zeroth-zeroth energy ($E_{0\text{-}0}$) of the dyes estimated from the intersection between the absorption and emission spectra, namely, HOMO$-E_{0\text{-}0}$. To effectively inject the electron into the CB of TiO_2, the LUMO levels of the dyes must be much more negative than the conducing band energy (E_{cb}) of semiconductor, −0.5 V (vs. NHE). From the LUMO values, it is clear that all of the dyes can achieve the electron injection and form the oxidized dyes.

Photovoltaic properties

The photovoltaic properties of these dyes for DSSCs are shown in Table 2 and *J-V* curves of the dyes are shown in Figure 5(a). An η value of 4.23% has been achieved (with short-circuit photo current density $J_{SC}=9.16$ mA/cm^2, open circuit photovoltage $V_{OC}=717$ mV, and fill factor $ff=0.64$) for DSSCs using S1P. The dyes S3O and S3P give η values of 3.94%, and 4.02%, respectively. Under similar experimental conditions, the N719 dye gives an η value of 5.90%. The dye S3P with longer alkoxy moieties shows higher open circuit photovoltage value than S1P, and S3O containing phenoxazine (POZ) unit shows the lowest open circuit photovoltage among the three dyes. The incident photon-to-current conversion efficiencies (IPCEs) of these dyes in DSSCs are shown in Figure 5(b). S3O gives broader IPCE spectra than S1P and S3P do in the spectral range of 350—750 nm. However, S1P gives higher IPCE value (up to 72% at 430 nm) than S3O and S3P do. Although the IPCE value of S3P is still lower than S1P,

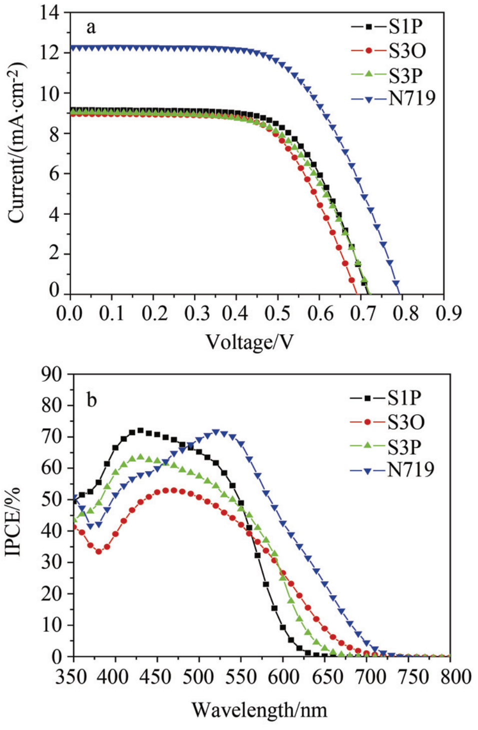

Figure 5 (a) Photocurrent density vs. voltage curves for DSSCs based on S1P, S3O, S3P and N719 under irradiation of AM 1.5G simulated solar light (100 mW•cm^{-2}). (b) The incident photon-to-current conversion efficiencies spectra for DSSCs based on S1P, S3O, S3P and N719.

© 2012 SIOC, CAS, Shanghai, & WILEY-VCH Verlag GmbH & Co. KGaA, Weinheim

Table 2 Photovoltaic performance of DSSCs based on S1P, S3O, S3P and N719 dyes[a]

Dye	J_{SC}/(mA•cm^{-2})	V_{OC}/mV	*ff*	*η*/%
S1P	9.16	717	0.64	4.23
S3O	8.96	691	0.64	3.94
S3P	9.05	721	0.62	4.02
N719	12.28	793	0.60	5.90

[a] Measured under irradiation of AM 1.5 G simulated solar light (100 mW•cm^{-2}) at room temperature, 12 μm film thickness, 0.25 cm^2 working area; electrolyte: 1.0 mol/L 1,2-dimethyl-3-*n*-propylimidazolium iodide (DMPII), 0.05 mol/L LiI, 0.03 mol/L I_2, 0.1 mol/L guanidinium thiocyanate (GuSCN), 0.5 mol/L 4-*tert*-butylpyridine (TBP) in AcCN and valeronitrile (85∶15); [b] The concentration of dyes is 3×10^{-4} mol/L in THF; [c] The concentration of N719 dye is 3×10^{-4} mol/L in ethanol.

the IPCE spectrum of S3P is broadened by modification with alkoxy groups. The results show that S3P and S3O have a broader absorption spectrum than S1P in dichloromethane solution because of the larger electron delocalization, and consequently lead to better photoelectric conversion properties to some extent. However, the photovoltaic conversion efficiency of S1P is higher than that of S3P and S3O due to the lower short-circuit current density. Therefore, it was found that the increase of electron donating ability is not always beneficial to improving the photoelectric conversion efficiency of DSSCs. These results agree well with the corresponding IPCE spectra.

Density functional theory (DFT) calculations were performed at a B3LYP/6-31G level for the geometry optimization to observe frontier molecular orbitals (MOs) of the HOMO and LUMO. The frontier MOs of all the dyes reveal that HOMO-LUMO excitation moves the electron density distribution from donor moieties to the cyanoacrylic acid acceptor (Figure 6). It is noteworthy that the LUMO electron density of all dyes is located mainly on the cyanoacrylic acid moiety. Therefore, the excited electron can be injected into the TiO_2 electrode efficiently.

Conclusions

In summary, we have synthesized three organic sensitizers with ethoxy-substituted oligo-phenylenevinylene as conjugation spacer and cyanoacrylic acid moiety as the electron acceptor. The three dyes were fully characterized and employed as sensitizers in dye sensitized solar cells. DSSCs sensitized by the S1P dye achieved a promising conversion efficiency of 4.23% under AM 1.5 100 mW/cm^2 illumination and had a high IPCE plateau of 72%, under similar experimental conditions, the N719 dye gives an *η* value of 5.90%. The dye S3O and S3P give broader IPCE spectra (reached to 750 nm for S3O). Structural modification of the S1P dye to improve the light absorption in the red and near-IR ranges for higher DSSCs performance is in progress.

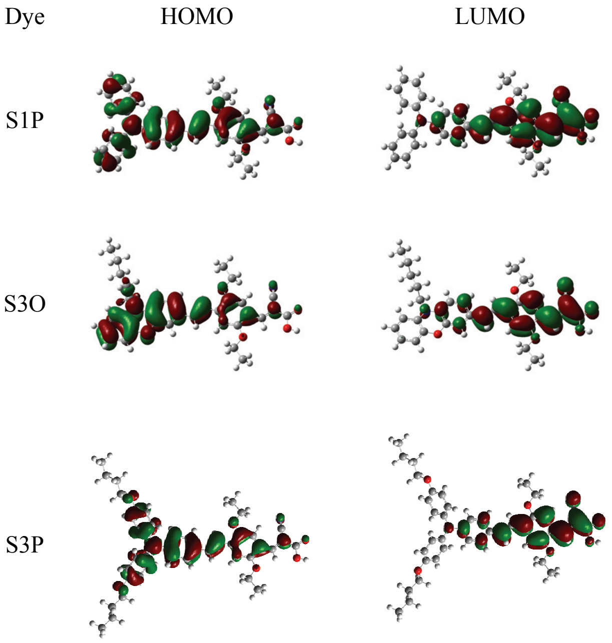

Figure 6 The frontier molecular orbitals (MOs) of the HOMO (left) and LUMO (right) of S1P, S3O and S3P.

Acknowledgement

We gratefully acknowledge the financial support of this work from Shanghai Committee of Science and Technology of China (No. 10520710100). We also thank the Laboratory of Organic Functional Molecules, Sino-French Institute of ECNU for support.

References

[1] O'Regan, B.; Grätzel, M. *Nature* **1991**, *353*, 737.

[2] Nazeeruddin, M. K.; Kay, A.; Rodicio, L.; Humpbry-Baker, R.; Miiller, E.; Liska, P.; Vlachopoulos, N.; Grätzel, M. *J. Am. Chem. Soc*. **1993**, *115*, 6382.

[3] Nazeeruddin, M. K.; Zakeeruddin, S. M.; Humphry-Baker, R.; Jirousek, M.; Liska, P.; Vlachopoulos, N.; Ahklover, V.; Fischer, C. H.; Grätzel, M. *Inorg. Chem*. **1999**, *38*, 6298.

[4] Nazeeruddin, M. K.; Péchy, P.; Renouard, T.; Zakeeruddin, S. M.; Humphry-Baker, R.; Comte, P.; Liska, P.; Cevey, L.; Costa, E.; Shklover, V.; Shklover, V.; Spiccia, L.; Deacon, G. B.; Bignozzi, C. A.; Grätzel, M. *J. Am. Chem. Soc*. **2001**, *123*, 1613.

[5] Gao, F.; Wang, Y.; Shi, D.; Zhang, J.; Wang, M.; Jing, X.; Humphry-Baker, R.; Wang, P.; Zakeeruddin, S. M.; Grätzel, M. *J. Am. Chem. Soc*. **2008**, *130*, 10720.

[6] Cao, Y. M.; Bai, Y.; Yu, Q. J.; Cheng, Y. M.; Liu, S.; Shi, D.; Gao, F. F.; Wang, P. *J. Phys. Chem. C*. **2009**, *113*, 6290.

[7] Chen, C. Y.; Wu, S. J.; Wu, C. G.; Chen, J. G.; Ho, K. C. *Angew. Chem., Int. Ed*. **2006**, *45*, 5822.

[8] Tian, H.; Yang, X.; Chen, R.; Pan, Y.; Li, L.; Hagfeldt, A.; Sun, L. *Chem. Commun*. **2007**, 3741.

[9] (a) Liu, B.; Zhu, W.; Zhang, Q.; Wu, W.; Xu, M.; Ning, Z.; Xie, Y.; Tian, H. *Chem. Commun*. **2009**, 1766; (b) Zhu, W. H.; Wu, Y. Z.; Wang, S. T.; Li, W. Q.; Li, X.; Chen, J.; Wang, Z. S.; Tian, H. *Adv. Funct. Mater*. **2011**, *21*, 756; (c) Ning, Z. J.; Tian, H. *Chem. Commun*. **2009**, 5283; (d) Ning, Z. J.; Fu, Y.; Tian, H. *Energy Environ. Sci*. **2010**, *3*, 1170; (e) He, J. X.; Wu, W. J.; Hua, J. L.; Jiang, Y. H.;

Qu, S. Y.; Li, J.; Long, Y. T.; Tian, H. *J. Mater. Chem.* **2011**, *21*, 6054.

[10] Zhou, G.; Pschirer, N.; Schoneboom, J. C.; Eickemeyer, F.; Baumgarten, M.; Müllen, K. *Chem. Mater.* **2008**, *20*, 1808.

[11] Zhang, J.; Li, H. B.; Wu, Y.; Geng, Y.; Duan, Y. A.; Liao, Y.; Su, Z. M. *Chem. J. Chin. Univ.* **2009**, *30*, 1343.

[12] Hao, Y.; Yang, X.; Cong, J.; Tian, H.; Hagfeldt, A.; Sun, L. *Chem. Commun.* **2009**, 4031 and references cited therein.

[13] Tao, L.; Yang, Y. Z.; Shi, C. W.; Wu, Y. C.; Wu, X. Y. *Acta Phys.-Chim. Sin.* **2010**, *26*, 578.

[14] Park, J. K.; Lee, H. R.; Chen, J. P.; Shinokubo, H.; Osuka, A.; Kim, D. *J. Phys. Chem. C* **2008**, *112*, 16691.

[15] Zhang, T. H.; Piao, L. Y.; Zhao, S. L.; Xu, Z.; Yang, L. A.; Liu, X. Z. *Chin. J. Org. Chem.* **2011**, *31*, 260 (in Chinese).

[16] (a) Shen, P.; Liu, Y. J.; Huang, X. W.; Zhao, B.; Xiang, N.; Fei, J. J.; Liu, L. M.; Wang, X. Y.; Huang, H.; Tan, S. T. *Dyes and Pigments* **2009**, *83*, 187; (b) Chen, H. J.; Huang, H.; Huang, X. W.; Clifford, N. J.; Forneli, A.; Palomares, E.; Zheng, X. Y.; Zheng, L. P.; Wang, X. Y.; Shen, P.; Zhao, B.; Tan, S. T. *J. Phys. Chem. C* **2010**, *114*, 3280; (d) Jiang, S. H.; Zhou, W. P.; Tan, Z.; Shen, P.; Zhao, B.; Tan, S. T. *Scientia Sinica Chimica* **2011**, *41*, 982; (e) Lu, M.; Liang, M.; Han, H. Y.; Sun, Z.; Xue, S. *J. Phys. Chem. C* **2011**, *115*, 274.

[17] Zhang, W. S.; Pan, S.; Li, Y. Z.; Chen, M. D. *Acta Phys.-Chim. Sin.* **2010**, *26*, 1408.

[18] Wang, Z.; Li, F.; Huang, C. *Chem. Commun.* **2000**, 2063.

[19] Tian, H.; Yang, X.; Chen, R.; Hagfeldt, A.; Sun, L. *Energy Environ. Sci.* **2009**, *2*, 674 and references cited therein.

[20] Zhang, L.; Liu, Y.; Wang, Z.; Liang, M.; Sun, Z.; Xue, S. *Tetrahedron* **2010**, *66*, 3318.

[21] Tang, K.; Liang, M.; Liu, Y.; Sun, Z.; Xue, S. *Chin. J. Chem.* **2011**, *29*, 89.

[22] Zhang, X. H.; Yao, Y. S.; Li, C.; Wang, W. B.; Cheng, X. X.; Wang, X. S.; Zhang, B. W. *Chin. J. Chem.* **2008**, *26*, 929.

[23] Teng, C.; Yang, X.; Yang, C.; Li, S.; Cheng, M.; Hagfeldt, A.; Sun, L. *J. Phys. Chem. C* **2010**, *114*, 9101 and references cited therein.

[24] Li, C.; Zhou, J. H.; Chen, J. R.; Chen, Y. S.; Zhang, X. H.; Ding, H. Y.; Wang, W. B.; Wang, X. S.; Zhang, B. W. *Chin. J. Chem.* **2006**, *24*, 537.

[25] Li, R.; Liu, J.; Cai, N.; Zhang, M.; Wang, P. *J. Phys. Chem. B*. **2010**, *114*, 4461 and references cited therein.

[26] Sun, S.; Xu, Y.; Liang, M.; Sun, Z.; Xue, S. *Chin. J. Org. Chem*. **2011**, *31*, 511 (in Chinese).

[27] Yella, A.; Lee, H.; Tsao, H. N.; Yi, C.; Chandiran, A. K.; Nazeeruddin, M. K.; Diau, E. W.; Yeh, C.; Zakeeruddin, S. M.; Grätzel, M. *Science* **2011**, *334*, 629.

[28] Gettinger, C. L.; Heeger, A. J.; Drakeand, J. M.; Pine, D. J. *Mol. Cryst. Liq. Cryst.* **1994**, *256*, 507.

[29] Herbert, M.; Dirk, I.; Ulf, S.; Kaloian, K.; Ayi, B.; Christoph, B. *Eur. J. Org. Chem.* **2001**, 4431.

[30] Nikolai, K.; Ana, L. P.; Giulia, M. R. *Org. Biomol. Chem.* **2005**, *3*, 524.

[31] Wang, Q.; Ito, S.; Grätzel, M.; Fabregat-Santiago, F.; Mora-Sero, I.; Bisquert, J.; Bessho, T.; Imai, H. *J. Phys. Chem. B* **2006**, *110*, 25210.

[32] Hagfeldt, A.; Grätzel, M. *Chem. Rev.* **1995**, *95*, 49.

[33] Zhang, M. D.; Pan, H.; Ju, X. H.; Ji, Y. J.; Qin, L.; Zheng, H. G.; Zhou, X. F. *Phys. Chem. Chem. Phys*. **2012**, *14*, 2809.

(Lu, Y.)

© 2012 SIOC, CAS, Shanghai, & WILEY-VCH Verlag GmbH & Co. KGaA, Weinheim